

Quantifying the Performance of Quantum Codes

Carlo Cafaro¹, Sonia L’Innocente², Cosmo Lupo³ and Stefano Mancini^{4,5}

^{1,3,4}*School of Science and Technology, Physics Division,
University of Camerino, I-62032 Camerino, Italy*

²*School of Science and Technology, Mathematics Division,
University of Camerino, I-62032 Camerino, Italy*

⁵*INFN, Sezione di Perugia, I-06123 Perugia, Italy*

We study the properties of error correcting codes for noise models in the presence of asymmetries and/or correlations by means of the entanglement fidelity and the code entropy. First, we consider a dephasing Markovian memory channel and characterize the performance of both a repetition code and an error avoiding code (\mathcal{C}_{RC} and \mathcal{C}_{DFS} , respectively) in terms of the entanglement fidelity. We also consider the concatenation of such codes ($\mathcal{C}_{DFS} \circ \mathcal{C}_{RC}$) and show that it is especially advantageous in the regime of partial correlations. Finally, we characterize the effectiveness of the codes \mathcal{C}_{DFS} , \mathcal{C}_{RC} and $\mathcal{C}_{DFS} \circ \mathcal{C}_{RC}$ by means of the code entropy and find, in particular, that the effort required for recovering such codes decreases when the error probability decreases and the memory parameter increases. Second, we consider both symmetric and asymmetric depolarizing noisy quantum memory channels and perform quantum error correction via the five qubit stabilizer code $\mathcal{C}_{[[5,1,3]]}$. We characterize this code by means of the entanglement fidelity and the code entropy as function of the asymmetric error probabilities and the degree of memory. Specifically, we uncover that while the asymmetry in the depolarizing errors does not affect the entanglement fidelity of the five qubit code, it becomes a relevant feature when the code entropy is used as a performance quantifier.

PACS numbers: Quantum Error Correction (03.67.Pp); Decoherence (03.65. Yz).

I. INTRODUCTION

Quantum error correction (QEC) is a theoretical scheme developed in quantum computing to defend quantum coherence against environmental noise. There are different methods for preserving quantum coherence. One possible technique exploits the redundancy in encoding information. This scheme is known as “quantum error correcting codes” (QECCs). For a comprehensive introduction to QECCs, we refer to [1]. Within such scheme, information is encoded in linear subspaces (codes) of the total Hilbert space in such a way that errors induced by the interaction with the environment can be detected and corrected. The QECC approach may be interpreted as an active stabilization of a quantum state in which, by monitoring the system and conditionally carrying on suitable operations, one prevents the loss of information. In detail, the errors occur on a qubit when its evolution differs from the ideal one. This happens by interaction of the qubit with an environment. Another possible approach is the so-called noiseless codes (also known as decoherence free subspaces (DFSs) or error avoiding codes). For a comprehensive introduction to DFSs, we refer to [2]. It turns out that for specific open quantum systems (noise models in which all qubits can be considered symmetrically coupled with the same environment), it is possible to design states that are hardly corrupted rather than states that can be easily corrected (in this sense, DFSs are complementary to QECCs). In other words, it is possible to encode information in linear subspaces such that the dynamics restricted to such subspaces is unitary. This implies that no information is lost and quantum coherence is maintained. DFS is an example of passive stabilization of quantum information.

The formal mathematical description of the qubit-environment interaction is usually given in terms of quantum channels. Quantum error correction is usually developed under the assumption of i.i.d. (identically and independently distributed) errors. These error models are characterized by memoryless channels Λ such that n -channel uses is given by $\Lambda^{(n)} = \Lambda^{\otimes n}$. In such cases of complete independent decoherence, qubits interact with their own environments which do not interact with each other. However, in many physical situations, qubits do interact with a common environment which unavoidably introduces correlations in the noise. For instance, there are situations where qubits in a ion trap set-up are collectively coupled to their vibrational modes [3]. In other situations, different qubits in a quantum dot design are coupled to the same lattice, thus interacting with a common thermal bath of phonons [4]. The exchange of bosons between qubits causes spatial and temporal correlations that violate the condition of error independence [5]. Memory effects then arise among channel uses with the consequence that $\Lambda^{(n)} \neq \Lambda^{\otimes n}$. Recent studies try to characterize the effect of correlations on the performance of QECCs [6–11]. It appears that correlations may have negative [7] or positive [8] impact on QECCs depending on the features of the error model being considered.

A part from being correlated, noise errors may also be asymmetric. Most of the quantum computing devices [12] are characterized by relaxation times ($\tau_{\text{relaxation}}$) that are one-two orders of magnitude larger than the corresponding

dephasing times ($\tau_{\text{dephasing}}$). Relaxation leads to both bit-flip and phase-flip errors, whereas dephasing (loss of phase coherence) only leads to phase-flip errors. Such asymmetry between $\tau_{\text{relaxation}}$ and $\tau_{\text{dephasing}}$ translates to an asymmetry in the occurrence probability of bit-flip (p_X) and phase-flip errors (p_Z). The ratio $\frac{p_Z}{p_X}$ is known as the channel asymmetry. Quantum error correction schemes should be designed in such a way that no resources (time and qubits) are wasted in attempting to detect and correct errors that may be relatively unlikely to occur. Quantum codes should be designed in order to exploit this asymmetry and provide better performance by neglecting the correction of less probable errors [13–15]. Indeed, examples of efficient quantum error-correcting codes taking advantage of this asymmetry are given by families of codes of the Calderbank-Shor-Steane (CSS) type (asymmetric stabilizer CSS codes) [16, 17].

Devising new good quantum codes for independent, correlated and asymmetric noise models is a highly non trivial problem. However, it is usually possible to manipulate in a smart way existing codes to construct new ones suitable for more general error models and with higher performances [18, 19]. Concatenation is perhaps one of the most successful quantum coding tricks employed to produce new codes from old ones. The concept of concatenated codes was first introduced in classical error correcting schemes by Forney [20]. Roughly speaking, concatenation is a method of combining two codes (an inner and an outer code) to form a larger code. In classical error correction, Forney has carried on extensive studies of concatenated codes, how to choose the inner and outer codes, and what error probability threshold values can be achieved. The first applications of concatenated codes in quantum error correction appear in [21, 22]. In the quantum setting, concatenated codes play a key role in fault tolerant quantum computation and in constructing good degenerate quantum error correcting codes.

Obviously enough, the choice of a code depends on the error model. However, in selecting a code rather than another, one should take into account their performance on the error model. Since there is no single quantity holding all information on a code, different quantum code performance quantifiers have appeared into the QEC literature [23]. For instance, in [24] it is suggested that the entanglement fidelity [25] is the important quantity to maximize in schemes for quantum error correction. In [26], it is proposed that the code entropy is an important quantitative measure of the quantum correction schemes by determining a hierarchical structure in the set of protected spaces [27].

Motivated by all the above mentioned considerations, in this work we study the properties of error correcting codes for noise models in the presence of asymmetries and/or correlations by means of the entanglement fidelity and the code entropy. First, we consider a dephasing Markovian memory channel and characterize the performance of both a repetition code and an error avoiding code (\mathcal{C}_{RC} and \mathcal{C}_{DFS} , respectively) in terms of the entanglement fidelity. We also consider the concatenation of such codes ($\mathcal{C}_{DFS} \circ \mathcal{C}_{RC}$) and show that it is especially advantageous in the regime of partial correlations. Finally, we characterize the effectiveness of the codes \mathcal{C}_{DFS} , \mathcal{C}_{RC} and $\mathcal{C}_{DFS} \circ \mathcal{C}_{RC}$ by means of the code entropy. We show that the effort required for recovering such codes decreases when the error probability decreases and/or the memory parameter increases. Second, we consider an asymmetric depolarizing noisy quantum memory channel and perform quantum error correction via the five qubit stabilizer code $\mathcal{C}_{[[5,1,3]]}$. We characterize this code by means of the entanglement fidelity and the code entropy as function of the asymmetric error probabilities and the degree of memory. Specifically, we uncover that while the asymmetry in the depolarizing errors does not affect the entanglement fidelity of the five qubit code, it becomes a relevant feature when quantifying the code performance by means of the code entropy.

The layout of this article is as follows. In Section II, we present few theoretical tools employed in the rest of the article. In particular, we emphasize the conceptual and operational meanings of the entanglement fidelity and code entropy, the two code performance quantifiers employed here. In Section III, we study a dephasing Markovian memory channel and characterize the performance of both a repetition code and an error avoiding code (\mathcal{C}_{RC} and \mathcal{C}_{DFS} , respectively) in terms of the entanglement fidelity. We also consider the concatenation of such codes ($\mathcal{C}_{DFS} \circ \mathcal{C}_{RC}$) and show that it is especially advantageous in the regime of partial correlations. Finally, we characterize the effectiveness of the codes \mathcal{C}_{DFS} , \mathcal{C}_{RC} and $\mathcal{C}_{DFS} \circ \mathcal{C}_{RC}$ by means of the code entropy. In Section IV, we analyze both symmetric and asymmetric depolarizing noisy quantum memory channels and perform quantum error correction via the five qubit stabilizer code $\mathcal{C}_{[[5,1,3]]}$. We characterize this code by means of the entanglement fidelity and the code entropy as function of the asymmetric error probabilities and the degree of memory. We find, among other things, that while asymmetric depolarizing errors do not affect the entanglement fidelity of the five qubit code, they do affect its code entropy. A summary of the uncovered results and our comments on the usefulness of both the entanglement fidelity and code entropy as suitable code performance quantifiers for the error models considered appear in Section V.

II. PRELIMINARIES

In this Section, we briefly describe some basic features of quantum error correcting codes and decoherence free subspaces. Finally, we point out the conceptual and operational meanings of the entanglement fidelity and code entropy, the two code performance quantifiers employed in this work.

A. On quantum error correction schemes

1. Quantum error correcting codes

The formal mathematical description of a system-environment interaction is usually given in terms of quantum channels [23]. When a quantum system in a state ρ (belonging to the set of density operators $\sigma(\mathcal{H})$ defined over the Hilbert space \mathcal{H} of dimension d associated to the system) is exposed to the interaction with the environment, the result is the noisy state describable by the action of a completely positive and trace preserving map $\Lambda : \sigma(\mathcal{H}) \rightarrow \sigma(\mathcal{H})$ with,

$$\Lambda(\rho) = \sum_k A_k \rho A_k^\dagger. \quad (1)$$

The operators $A_k : \mathcal{H} \rightarrow \mathcal{H}$ (Kraus operators) define the errors affecting the system's state ρ . It is well known [23] that a standard quantum error correction scheme is characterized by a subspace $\mathcal{C} \subseteq \mathcal{H}$ such that for some Hermitian and positive matrix of complex scalars $\Gamma = (\gamma_{lm})$ the corresponding projection operator $P_{\mathcal{C}}$ fulfills the error correction condition,

$$P_{\mathcal{C}} A_l^\dagger A_m P_{\mathcal{C}} = \gamma_{lm} P_{\mathcal{C}}, \quad (2)$$

for $l, m = 1, \dots, d^2$. The matrix Γ is also known as the error correction matrix. The action of the correctable error operators $\{A\}_{\text{correctable}} \subseteq \{A_k\}$ on vectors spanning \mathcal{C} (codewords) allows to define the (completely positive and trace preserving) recovery map $\mathcal{R} \leftrightarrow \{R_l\}$. The composition of the recovery map \mathcal{R} with the error map \mathcal{A} gives the recovered channel,

$$\Lambda_{\text{rec.}}(\rho) \stackrel{\text{def}}{=} (\mathcal{R} \circ \Lambda)(\rho) = \sum_l \sum_k (R_l A_k) \rho (R_l A_k)^\dagger. \quad (3)$$

For a comprehensive introduction to QECCs, we refer to [1].

2. Decoherence Free Subspaces

Following [2], we mention few relevant properties of DFSs. Consider the dynamics of a closed system composed of a quantum system \mathcal{Q} coupled to a bath \mathcal{B} . The unitary evolution of the closed system is described by the combined system-bath Hamiltonian H_{tot} , $H_{\text{tot}} = H_{\mathcal{Q}} \otimes I_{\mathcal{B}} + H_{\mathcal{B}} \otimes I_{\mathcal{Q}} + H_{\text{int}}$, $H_{\text{int}} = \sum_{\alpha} E_{\alpha} \otimes B_{\alpha}$. The operator $H_{\mathcal{Q}}$ ($H_{\mathcal{B}}$) is the system (bath) Hamiltonian, $I_{\mathcal{Q}}$ ($I_{\mathcal{B}}$) is the identity operator of the system (bath), E_{α} are the error generators acting solely on \mathcal{Q} while B_{α} act on the bath. The last term in H_{tot} is the interaction Hamiltonian.

A subspace \mathcal{H}_{DFS} of the total system Hilbert space \mathcal{H} is a decoherence free subspace if and only if: i) $E_{\alpha} |\psi\rangle = c_{\alpha} |\psi\rangle$ with $c_{\alpha} \in \mathbb{C}$, for all states $|\psi\rangle$ spanning \mathcal{H}_{DFS} , and for every error operator E_{α} in H_{int} . In other words, all basis states spanning \mathcal{H}_{DFS} are degenerate eigenstates of all the error generators E_{α} ; ii) \mathcal{Q} and \mathcal{B} are initially decoupled; iii) $H_{\mathcal{Q}} |\psi\rangle$ has no overlap with states in the subspace orthogonal to \mathcal{H}_{DFS} . To establish a direct link between QECCs and DFSs, it is more convenient to present an alternative formulation of DFSs in terms of the Kraus operator sum representation. Within such description, the evolution of the system \mathcal{Q} density matrix is written as, $\rho_{\mathcal{Q}}(t) = \text{Tr}_{\mathcal{B}} [U(\rho_{\mathcal{Q}} \otimes \rho_{\mathcal{B}})U^\dagger] = \sum_k A_k \rho_{\mathcal{Q}}(0) A_k^\dagger$, where $U = e^{-iH_{\text{tot}}t}$ is the unitary evolution operator for the system-bath closed system and the initial bath density matrix $\rho_{\mathcal{B}}$ equals $\sum_n \lambda_n |n\rangle \langle n|$. The Kraus operators A_k (satisfying the normalization condition) are given by $A_k = \sqrt{\lambda_n} \langle m|U|n\rangle$ with $\sum_k A_k^\dagger A_k = I_{\mathcal{Q}}$ with $k = (n, m)$ and where $|m\rangle$ and $|n\rangle$ are bath states. It turns out that a N_{DFS} -dimensional subspace \mathcal{H}_{DFS} of \mathcal{H} is a DFS if and only if all Kraus operators have an identical unitary representation (in the basis where the first N_{DFS} states span \mathcal{H}_{DFS}) upon restriction to it, up to a multiplicative constant,

$$A_k = \begin{pmatrix} g_k U_{\mathcal{Q}}^{(\text{DFS})} & 0 \\ 0 & \bar{A}_k \end{pmatrix}, \quad (4)$$

where $g_k = \sqrt{\lambda_n} \langle m|U_c|n\rangle$ and $U_c = e^{-iH_c t}$ with $H_c = H_{\mathcal{B}} + H_{\text{int}}$. Furthermore, \bar{A}_k is an arbitrary matrix that acts on $\mathcal{H}_{\text{DFS}}^\perp$ (with $\mathcal{H} = \mathcal{H}_{\text{DFS}} \oplus \mathcal{H}_{\text{DFS}}^\perp$) and may cause decoherence there; $U_{\mathcal{Q}}^{(\text{DFS})}$ is $U_{\mathcal{Q}}$ restricted to \mathcal{H}_{DFS} . Now recall that in ordinary QECCs, it is possible to correct the errors induced by a given set of Kraus operators $\{A_k\}$ if and only if,

$$R_r A_k = \begin{pmatrix} \lambda_{rk} I_{\mathcal{C}} & 0 \\ 0 & B_{rk} \end{pmatrix}, \quad (5)$$

$\forall r$ and k , or equivalently,

$$A_k^\dagger A_{k'} = \begin{pmatrix} \gamma_{kk'} I_{\mathcal{C}} & 0 \\ 0 & \bar{A}_k^\dagger \bar{A}_{k'} \end{pmatrix}, \quad (6)$$

where $\{R_r\}$ are the recovery operators. The first block in the RHS of (5) acts on the code space \mathcal{C} while the matrices B_{rk} act on \mathcal{C}^\perp where $\mathcal{H} = \mathcal{C} \oplus \mathcal{C}^\perp$. From (4) and (5), it follows that DFS can be viewed as a special class of QECCs, where upon restriction to the code space \mathcal{C} , all recovery operators R_r are proportional to the inverse of the system \mathcal{Q} evolution operator, $R_r \propto \left(U_{\mathcal{Q}}^{(\text{DFS})}\right)^\dagger$. Assuming that R_r is proportional to the dagger of $U_{\mathcal{Q}}^{(\text{DFS})}$, from (4) and (6) it also turns out that $A_k \propto U_{\mathcal{Q}}^{(\text{DFS})}$ upon restriction to \mathcal{C} . Furthermore, from (4) and (6), it follows that $\gamma_{kk'} = g_k^* g_{k'}$. However, while in the QECCs case $\gamma_{kk'}$ is in general a full-rank matrix (non-degenerate code), in the DFSs case this matrix has rank 1. In conclusion, a DFS can be viewed as a special type of QECC, namely a completely degenerate quantum error correcting code where upon restriction to the code subspace all recovery operators are proportional to the inverse of the system evolution operator. As a side remark, in view of this last observation we point out that it is reasonable to quantify the performance of both active and passive QEC schemes by means of the same performance measure. In what follows, we will briefly describe the conceptual and operational meanings of the entanglement fidelity and code entropy, respectively.

B. On code performance quantifiers: entanglement fidelity and code entropy

1. Entanglement Fidelity

Entanglement fidelity is a useful measure of the efficiency of QECCs. It is a quantity that keeps track of how well the state and entanglement of a subsystem of a larger system are stored, without requiring the knowledge of the complete state or dynamics of the larger system. More precisely, the entanglement fidelity is defined for a mixed state $\rho = \sum_i p_i \rho_i = \text{tr}_{\mathcal{H}_R} |\psi\rangle\langle\psi|$ in terms of a purification $|\psi\rangle \in \mathcal{H} \otimes \mathcal{H}_R$ to a reference system \mathcal{H}_R . The purification $|\psi\rangle$ encodes all of the information in ρ . Entanglement fidelity is a measure of how well the channel Λ preserves the entanglement of the state \mathcal{H} with its reference system \mathcal{H}_R . The entanglement fidelity is formally defined as follows [25],

$$\mathcal{F}(\rho, \Lambda) \stackrel{\text{def}}{=} \langle\psi| (\Lambda \otimes I_{\mathcal{H}_R}) (|\psi\rangle\langle\psi|) |\psi\rangle, \quad (7)$$

where $|\psi\rangle$ is any purification of ρ , $I_{\mathcal{H}_R}$ is the identity map on $\sigma(\mathcal{H}_R)$ and $\Lambda \otimes I_{\mathcal{H}_R}$ is the evolution operator extended to the space $\mathcal{H} \otimes \mathcal{H}_R$, space on which ρ has been purified. If the quantum operation Λ is written in terms of its Kraus operator elements $\{A_k\}$ as, $\Lambda(\rho) = \sum_k A_k \rho A_k^\dagger$, then it can be shown that the operational expression of (7) becomes [24],

$$\mathcal{F}(\rho, \Lambda) = \sum_k \text{tr}(A_k \rho) \text{tr}(A_k^\dagger \rho) = \sum_k |\text{tr}(\rho A_k)|^2. \quad (8)$$

This expression for the entanglement fidelity is very useful for explicit calculations. Finally, assuming that

$$\Lambda : \sigma(\mathcal{H}) \ni \rho \mapsto \Lambda(\rho) = \sum_k A_k \rho A_k^\dagger \in \sigma(\mathcal{H}), \dim_{\mathbb{C}} \mathcal{H} = N \quad (9)$$

and choosing a purification described by a maximally entangled unit vector $|\psi\rangle \in \mathcal{H} \otimes \mathcal{H}$ for the mixed state $\rho = \frac{1}{\dim_{\mathbb{C}} \mathcal{H}} I_{\mathcal{H}}$, we obtain

$$\mathcal{F}\left(\frac{1}{N} I_{\mathcal{H}}, \Lambda\right) = \frac{1}{N^2} \sum_k |\text{tr} A_k|^2. \quad (10)$$

The expression in (10) represents the entanglement fidelity when no error correction is performed on the noisy channel Λ in (9).

2. Code entropy

A convenient quantifier of the action of the map Λ in (1) on a initial quantum state ρ is represented by the entropy change $\mathcal{S}(\Lambda(\rho)) - \mathcal{S}(\rho)$. It can be shown that [28],

$$0 \leq |\mathcal{S}(\Lambda(\rho)) - \mathcal{S}(\sigma)| \leq \mathcal{S}(\rho) \leq \mathcal{S}(\Lambda(\rho)) + \mathcal{S}(\sigma), \quad (11)$$

where $\sigma = \sigma(\Lambda, \rho)$ is the so-called Lindblad matrix, an auxiliary quantum state with matrix elements σ_{lm} defined as,

$$\sigma_{lm} \stackrel{\text{def}}{=} \text{Tr}(\rho A_l^\dagger A_m), \quad (12)$$

with $l, m = 1, 2, \dots, d^2$. The bounds provided in (11) are the so-called Lindblad bounds [28]. The quantity $\mathcal{S}(\sigma)$ is known as the entropy exchange of the operation Λ . From (11), it follows that if ρ is pure, $\mathcal{S}(\rho) = 0$ and therefore $\mathcal{S}(\sigma) = \mathcal{S}(\Lambda(\rho))$.

As pointed out earlier, a standard quantum error correction scheme for a given quantum operation Λ is characterized by a subspace \mathcal{C} such that for some Hermitian and positive error correction matrix of complex scalars $\Gamma = (\gamma_{lm})$ the corresponding projection operator fulfills the relation (2). A quantum error correcting code for Λ is determined by the subspace related to $P_{\mathcal{C}}$. The rank of Γ is bounded above by the dynamical Choi matrix \mathcal{D}_Λ associated with $\Lambda(\rho)$,

$$\mathcal{D}_\Lambda \stackrel{\text{def}}{=} \text{Tr}(A_l^\dagger A_m). \quad (13)$$

For orthogonal Kraus operators $\{A_l\}$, the Choi matrix equals $d_l \delta_{lm}$ with $0 \leq d_l$ representing the eigenvalues of \mathcal{D}_Λ . The rank of \mathcal{D}_Λ equals the minimal number of Kraus operators needed to describe Λ . Given a code \mathcal{C} for Λ and assuming that the initial quantum state ρ belongs to the code subspace (that is, $P_{\mathcal{C}}\rho P_{\mathcal{C}} = \rho$), it turns out that $\sigma_{lm} = \gamma_{lm}$ [26]. In other words, the error correction matrix Γ equals the Lindblad matrix $\sigma(\Lambda, \rho)$ provided that the initial quantum state ρ belongs to the code subspace. Motivated by these considerations, given a quantum operation Λ with Kraus operators $\{A_l\}$ and a code \mathcal{C} with error correction matrix Γ , Kribs and coworkers named the von Neumann entropy $\mathcal{S}(\Lambda, \mathcal{C})$,

$$\mathcal{S}(\Lambda, \mathcal{C}) \stackrel{\text{def}}{=} \mathcal{S}(\Gamma) = -\text{Tr}(\Gamma \log \Gamma), \quad (14)$$

the entropy of \mathcal{C} relative to Λ [26]. They show that,

$$0 \leq \mathcal{S}(\Lambda, \mathcal{C}) \leq \log D, \quad (15)$$

where $\mathcal{S}(\Lambda, \mathcal{C}) = 0$ iff \mathcal{C} is a unitarily correctable code for Λ and $\mathcal{S}(\Lambda, \mathcal{C}) = \log D$ iff \mathcal{C} is a non-degenerate code for Λ . From a conceptual point of view, the entropy of a code \mathcal{C} relative to a quantum noisy channel Λ can be viewed as a measure quantifying the nearness of the given error correcting code \mathcal{C} to a decoherence free subspace C_{DFS} . The closer \mathcal{C} is to a C_{DFS} , the smaller is the code entropy $\mathcal{S}(\Lambda, \mathcal{C})$. The smaller is the code entropy, the smaller is the amount of effort required to recover the quantum state corrupted by the noise by means of a suitable error recovery operation. The simplest scenario occurs for codes with zero entropy. Such codes are known, as we said, as unitarily correctable codes and can be recovered with a single unitary operation. In particular decoherence free subspaces are a special class of unitarily correctable codes where the recovery is given by the trivial identity operation.

We recall that in standard active error correction schemes, the action of the recovery operation pushes all the noise into the ancillary qubits, so that errors are eliminated when the ancilla is traced out [29]. That said, we emphasize that the numerical value of the code entropy quantifies the number of ancilla qubits needed to perform a recovery operation [26] and the rank of Γ gives the number of Kraus operators necessary to describe the action of Λ restricted to \mathcal{C} and therefore the number of Kraus operators necessary for a recovery operation.

III. MODEL I: DEPHASING MARKOVIAN MEMORY CHANNEL

In this Section, we consider a dephasing Markovian memory channel and characterize the performance of both a repetition code and an error avoiding code (\mathcal{C}_{RC} and \mathcal{C}_{DFS} , respectively) in terms of the entanglement fidelity. In particular, we consider the concatenation of such codes ($\mathcal{C}_{DFS} \circ \mathcal{C}_{RC}$) and show that it is especially advantageous in the regime of partial correlations. Finally, we characterize the effectiveness of the codes \mathcal{C}_{DFS} , \mathcal{C}_{RC} and $\mathcal{C}_{DFS} \circ \mathcal{C}_{RC}$ by means of the code entropy. We show that the effort required for recovering such codes decreases when the error probability decreases and the memory parameter increases.

A. Entanglement fidelity-based analysis

Repetition code for correlated phase flips. The model considered is a dephasing quantum Markovian memory channel $\Lambda^{(n)}(\rho)$. In explicit terms, we consider n qubits and Markovian correlated errors in a dephasing quantum channel,

$$\Lambda^{(n)}(\rho) \stackrel{\text{def}}{=} \sum_{i_1, \dots, i_n=0}^1 p_{i_n|i_{n-1}} p_{i_{n-1}|i_{n-2}} \dots p_{i_2|i_1} p_{i_1} (A_{i_n} \otimes \dots \otimes A_{i_1}) \rho (A_{i_n} \otimes \dots \otimes A_{i_1})^\dagger, \quad (16)$$

where $A_0 \stackrel{\text{def}}{=} I$, $A_1 \stackrel{\text{def}}{=} Z$ are Pauli operators. Furthermore the conditional probabilities $p_{i_k|i_{k-1}}$ are given by,

$$p_{i_k|i_{k-1}} = (1 - \mu)p_{i_k} + \mu\delta_{i_k, i_{k-1}}, \quad p_{i_k=0} = 1 - p, p_{i_k=1} = p, \quad (17)$$

with,

$$\sum_{i_1, \dots, i_n=0}^1 p_{i_n|i_{n-1}} p_{i_{n-1}|i_{n-2}} \dots p_{i_2|i_1} p_{i_1} = 1. \quad (18)$$

To simplify our notation, we may choose to omit the symbol of tensor product " \otimes " in the future, $A_{i_n} \otimes \dots \otimes A_{i_1} \equiv A_{i_n} \dots A_{i_1}$. Furthermore, we may choose to omit the bar " $|$ " in $p_{i_k|i_j}$ and simply write the conditional probabilities as $p_{i_k i_j}$. QEC is performed via the three-qubit repetition code. Although the error model considered is not truly quantum, we can gain useful insights for extending error correction techniques to fully quantum error models in the presence of partial correlations. The performance of quantum error correcting codes is quantified by means of the entanglement fidelity as function of the error probability p and degree of memory μ . By considering the case of (16) with $n = 3$, it follows that the error superoperator \mathcal{A} associated to channel is defined in terms of the following error operators,

$$\mathcal{A} \longleftrightarrow \{A'_0, \dots, A'_7\} \text{ with } \Lambda^{(3)}(\rho) \stackrel{\text{def}}{=} \sum_{k=0}^7 A'_k \rho A_k^\dagger \text{ and, } \sum_{k=0}^7 A_k'^\dagger A'_k = I_{8 \times 8}. \quad (19)$$

In an explicit way, the error operators $\{A'_0, \dots, A'_7\}$ are given by,

$$\begin{aligned} A'_0 &= \sqrt{\tilde{p}_0^{(3)}} I^1 \otimes I^2 \otimes I^3, A'_1 = \sqrt{\tilde{p}_1^{(3)}} Z^1 \otimes I^2 \otimes I^3, A'_2 = \sqrt{\tilde{p}_2^{(3)}} I^1 \otimes Z^2 \otimes I^3, \\ A'_3 &= \sqrt{\tilde{p}_3^{(3)}} I^1 \otimes I^2 \otimes Z^3, A'_4 = \sqrt{\tilde{p}_4^{(3)}} Z^1 \otimes Z^2 \otimes I^3, A'_5 = \sqrt{\tilde{p}_5^{(3)}} Z^1 \otimes I^2 \otimes Z^3, \\ A'_6 &= \sqrt{\tilde{p}_6^{(3)}} I^1 \otimes Z^2 \otimes Z^3, A'_7 = \sqrt{\tilde{p}_7^{(3)}} Z^1 \otimes Z^2 \otimes Z^3, \end{aligned} \quad (20)$$

where the coefficients $\tilde{p}_k^{(3)}$ for $k = 1, \dots, 7$ read,

$$\begin{aligned} \tilde{p}_0^{(3)} &= p_{00}^2 p_0, \tilde{p}_1^{(3)} = p_{00} p_{10} p_0, \tilde{p}_2^{(3)} = p_{01} p_{10} p_0, \tilde{p}_3^{(3)} = p_{00} p_{01} p_1, \\ \tilde{p}_4^{(3)} &= p_{10} p_{11} p_0, \tilde{p}_5^{(3)} = p_{01} p_{10} p_1, \tilde{p}_6^{(3)} = p_{01} p_{11} p_1, \tilde{p}_7^{(3)} = p_{11}^2 p_1, \end{aligned} \quad (21)$$

with,

$$\begin{aligned} p_0 &= (1 - p), p_1 = p, p_{00} = ((1 - \mu)(1 - p) + \mu), \\ p_{01} &= (1 - \mu)(1 - p), p_{10} = (1 - \mu)p, p_{11} = ((1 - \mu)p + \mu). \end{aligned} \quad (22)$$

Then consider a repetition code that encodes 1 logical qubit into 3-physical qubits. The codewords are given by,

$$|0\rangle \rightarrow |0_L\rangle \stackrel{\text{def}}{=} |+++\rangle, |1\rangle \rightarrow |1_L\rangle \stackrel{\text{def}}{=} |--\rangle, \quad (23)$$

where $|\pm\rangle \stackrel{\text{def}}{=} \frac{|0\rangle \pm |1\rangle}{\sqrt{2}}$. The set of error operators satisfying the detectability condition [30], $P_C A'_k P_C = \lambda_{A'_k} P_C$, where $P_C = |0_L\rangle\langle 0_L| + |1_L\rangle\langle 1_L|$ is the projector operator on the code subspace $\mathcal{C} = \text{Span}\{|0_L\rangle, |1_L\rangle\}$ is given by,

$$\mathcal{A}_{\text{detectable}} = \{A'_0, A'_1, A'_2, A'_3, A'_4, A'_5, A'_6\} \subseteq \mathcal{A}. \quad (24)$$

The only non-detectable error is A'_7 . Furthermore, since all the detectable errors are invertible, the set of correctable errors is such that $\mathcal{A}_{\text{correctable}}^\dagger \mathcal{A}_{\text{correctable}}$ is detectable. It follows then that,

$$\mathcal{A}_{\text{correctable}} = \{A'_0, A'_1, A'_2, A'_3\} \subseteq \mathcal{A}_{\text{detectable}} \subseteq \mathcal{A}. \quad (25)$$

The action of the correctable error operators $\mathcal{A}_{\text{correctable}}$ on the codewords $|0_L\rangle$ and $|1_L\rangle$ is given by,

$$\begin{aligned} |0_L\rangle &\rightarrow A'_0 |0_L\rangle = \sqrt{\tilde{p}_0^{(3)}} |+++\rangle, A'_1 |0_L\rangle = \sqrt{\tilde{p}_1^{(3)}} |-++\rangle, A'_2 |0_L\rangle = \sqrt{\tilde{p}_2^{(3)}} |+-+\rangle, A'_3 |0_L\rangle = \sqrt{\tilde{p}_3^{(3)}} |++-\rangle \\ |1_L\rangle &\rightarrow A'_0 |1_L\rangle = \sqrt{\tilde{p}_0^{(3)}} |--\rangle, A'_1 |1_L\rangle = \sqrt{\tilde{p}_1^{(3)}} |+-\rangle, A'_2 |1_L\rangle = \sqrt{\tilde{p}_2^{(3)}} |-+-\rangle, A'_3 |1_L\rangle = \sqrt{\tilde{p}_3^{(3)}} |--+\rangle \end{aligned} \quad (26)$$

The two four-dimensional orthogonal subspaces \mathcal{V}^{0_L} and \mathcal{V}^{1_L} of \mathcal{H}_2^3 generated by the action of $\mathcal{A}_{\text{correctable}}$ on $|0_L\rangle$ and $|1_L\rangle$ result,

$$\mathcal{V}^{0_L} = \text{Span} \{ |v_1^{0_L}\rangle = |+++\rangle, |v_2^{0_L}\rangle = |-++\rangle, |v_3^{0_L}\rangle = |+-+\rangle, |v_4^{0_L}\rangle = |++-\rangle \}, \quad (27)$$

and,

$$\mathcal{V}^{1_L} = \text{Span} \{ |v_1^{1_L}\rangle = |--\rangle, |v_2^{1_L}\rangle = |+-\rangle, |v_3^{1_L}\rangle = |-+-\rangle, |v_4^{1_L}\rangle = |--+\rangle \}, \quad (28)$$

respectively. Notice that $\mathcal{V}^{0_L} \oplus \mathcal{V}^{1_L} = \mathcal{H}_2^3$. The recovery superoperator $\mathcal{R} \leftrightarrow \{R_l\}$ with $l = 1, \dots, 4$ is defined as [31],

$$R_l \stackrel{\text{def}}{=} V_l \sum_{i=0}^1 |v_l^{i_L}\rangle \langle v_l^{i_L}|, \quad (29)$$

where the unitary operator V_l is such that $V_l |v_l^{i_L}\rangle = |i_L\rangle$ for $i \in \{0, 1\}$. Substituting (27) and (28) into (29), it follows that the four recovery operators $\{R_1, R_2, R_3, R_4\}$ are given by,

$$\begin{aligned} R_1 &= |0_L\rangle \langle 0_L| + |1_L\rangle \langle 1_L|, R_2 = |0_L\rangle \langle -++| + |1_L\rangle \langle +-+|, \\ R_3 &= |0_L\rangle \langle +-+| + |1_L\rangle \langle -+-|, R_4 = |0_L\rangle \langle +++| + |1_L\rangle \langle --+|. \end{aligned} \quad (30)$$

Using simple algebra, it turns out that the 8×8 matrix representation $[R_l]$ with $l = 1, \dots, 4$ of the recovery operators is given by,

$$[R_1] = E_{11} + E_{88}, [R_2] = E_{12} + E_{87}, [R_3] = E_{13} + E_{86}, [R_4] = E_{14} + E_{85}, \quad (31)$$

where E_{ij} is the 8×8 matrix where the only non-vanishing element is the one located in the ij -position and it equals 1. The action of this recovery operation \mathcal{R} on the map $\Lambda^{(3)}(\rho)$ in (19) leads to,

$$\Lambda_{\text{recover}}^{(3)}(\rho) \equiv \left(\mathcal{R} \circ \Lambda^{(3)} \right)(\rho) \stackrel{\text{def}}{=} \sum_{k=0}^7 \sum_{l=1}^4 (R_l A'_k) \rho (R_l A'_k)^\dagger. \quad (32)$$

We want to describe the action of $\mathcal{R} \circ \Lambda^{(3)}$ restricted to the code subspace \mathcal{C} . Therefore, we compute the 2×2 matrix representation $[R_l A'_k]_{|\mathcal{C}}$ of each $R_l A'_k$ with $l = 1, \dots, 4$ and $k = 0, \dots, 7$ where,

$$[R_l A'_k]_{|\mathcal{C}} \stackrel{\text{def}}{=} \begin{pmatrix} \langle 0_L | R_l A'_k | 0_L \rangle & \langle 0_L | R_l A'_k | 1_L \rangle \\ \langle 1_L | R_l A'_k | 0_L \rangle & \langle 1_L | R_l A'_k | 1_L \rangle \end{pmatrix}. \quad (33)$$

Substituting (26) and (30) into (33), it turns out that the only matrices $[R_l A'_k]_{|\mathcal{C}}$ with non-vanishing trace are given by,

$$\begin{aligned} [R_1 A'_0]_{|\mathcal{C}} &= \sqrt{\tilde{p}_0^{(3)}} \begin{pmatrix} 1 & 0 \\ 0 & 1 \end{pmatrix}, [R_2 A'_1]_{|\mathcal{C}} = \sqrt{\tilde{p}_1^{(3)}} \begin{pmatrix} 1 & 0 \\ 0 & 1 \end{pmatrix}, \\ [R_3 A'_2]_{|\mathcal{C}} &= \sqrt{\tilde{p}_2^{(3)}} \begin{pmatrix} 1 & 0 \\ 0 & 1 \end{pmatrix}, [R_4 A'_3]_{|\mathcal{C}} = \sqrt{\tilde{p}_3^{(3)}} \begin{pmatrix} 1 & 0 \\ 0 & 1 \end{pmatrix}. \end{aligned} \quad (34)$$

Therefore, the entanglement fidelity $\mathcal{F}_{\text{phase}}^{(3)}(\mu, p)$ defined as,

$$\mathcal{F}_{\text{phase}}^{(3)}(\mu, p) \stackrel{\text{def}}{=} \mathcal{F}^{(3)}\left(\frac{1}{2}I_{2 \times 2}, \mathcal{R} \circ \Lambda^{(3)}\right) = \frac{1}{(2)^2} \sum_{k=0}^7 \sum_{l=1}^4 \left| \text{tr}([R_l A'_k]_{\mathcal{C}}) \right|^2, \quad (35)$$

results,

$$\mathcal{F}_{\text{phase}}^{(3)}(\mu, p) = \mu^2 (2p^3 - 3p^2 + p) + \mu (-4p^3 + 6p^2 - 2p) + (2p^3 - 3p^2 + 1). \quad (36)$$

DFS for correlated phase flips. By considering the case of (16) with $n = 2$ qubits it follows that the error superoperator \mathcal{A} associated to channel is defined in terms of the following error operators,

$$\mathcal{A} \longleftrightarrow \{A'_0, \dots, A'_3\} \text{ with } \Lambda^{(2)}(\rho) \stackrel{\text{def}}{=} \sum_{k=0}^3 A'_k \rho A'_k{}^\dagger \text{ and, } \sum_{k=0}^3 A'_k{}^\dagger A'_k = I_{4 \times 4}. \quad (37)$$

In an explicit way, the error operators $\{A'_0, \dots, A'_3\}$ are given by,

$$A'_0 = \sqrt{\tilde{p}_0^{(2)}} I^1 \otimes I^2, A'_1 = \sqrt{\tilde{p}_1^{(2)}} Z^1 \otimes I^2, A'_2 = \sqrt{\tilde{p}_2^{(2)}} I^1 \otimes Z^2, A'_3 = \sqrt{\tilde{p}_3^{(2)}} Z^1 \otimes Z^2, \quad (38)$$

where the coefficients $\tilde{p}_k^{(2)}$ for $k = 0, \dots, 3$ read,

$$\tilde{p}_0^{(2)} = p_{00}p_0, \tilde{p}_1^{(2)} = p_{10}p_0, \tilde{p}_2^{(2)} = p_{01}p_1, \tilde{p}_3^{(2)} = p_{11}p_1. \quad (39)$$

We encode our logical qubit with a simple decoherence free subspace of two qubits given by [2],

$$|0\rangle \longrightarrow |0_L\rangle \stackrel{\text{def}}{=} |01\rangle \text{ and, } |1\rangle \longrightarrow |1_L\rangle \stackrel{\text{def}}{=} |10\rangle. \quad (40)$$

The set of error operators satisfying the detectability condition [30], $P_{\mathcal{C}} A'_k P_{\mathcal{C}} = \lambda_{A'_k} P_{\mathcal{C}}$, where $P_{\mathcal{C}} = |0_L\rangle\langle 0_L| + |1_L\rangle\langle 1_L|$ is the projector operator on the code subspace $\mathcal{C} = \text{Span}\{|0_L\rangle, |1_L\rangle\}$ is given by,

$$\mathcal{A}_{\text{detectable}} = \{A'_0, A'_3\} \subseteq \mathcal{A}. \quad (41)$$

Furthermore, since all the detectable errors are invertible, the set of correctable errors is such that $\mathcal{A}_{\text{correctable}}^\dagger \mathcal{A}_{\text{correctable}}$ is detectable. It follows then that,

$$\mathcal{A}_{\text{correctable}} = \mathcal{A}_{\text{detectable}} \subseteq \mathcal{A}. \quad (42)$$

The action of the correctable error operators $\mathcal{A}_{\text{correctable}}$ on the codewords $|0_L\rangle$ and $|1_L\rangle$ is given by,

$$|0_L\rangle \rightarrow A'_0 |0_L\rangle = \sqrt{\tilde{p}_0^{(2)}} |01\rangle, A'_3 |0_L\rangle = -\sqrt{\tilde{p}_3^{(2)}} |01\rangle, |1_L\rangle \rightarrow A'_0 |1_L\rangle = \sqrt{\tilde{p}_0^{(2)}} |10\rangle, A'_3 |1_L\rangle = -\sqrt{\tilde{p}_3^{(2)}} |10\rangle. \quad (43)$$

The two one-dimensional orthogonal subspaces \mathcal{V}^{0_L} and \mathcal{V}^{1_L} of \mathcal{H}_2^2 generated by the action of $\mathcal{A}_{\text{correctable}}$ on $|0_L\rangle$ and $|1_L\rangle$ are given by,

$$\mathcal{V}^{0_L} = \text{Span}\{|v_1^{0_L}\rangle = |01\rangle\} \text{ and, } \mathcal{V}^{1_L} = \text{Span}\{|v_1^{1_L}\rangle = |10\rangle\}. \quad (44)$$

Notice that $\mathcal{V}^{0_L} \oplus \mathcal{V}^{1_L} \neq \mathcal{H}_2^2$. This means that the trace preserving recovery superoperator \mathcal{R} is defined in terms of one standard recovery operator R_1 and by the projector R_\perp onto the orthogonal complement of $\bigoplus_{i=0}^1 \mathcal{V}^{i_L}$, i. e. the part of the Hilbert space \mathcal{H}_2^2 which is not reached by acting on the code \mathcal{C} with the correctable error operators. In the case under consideration,

$$R_1 \stackrel{\text{def}}{=} |01\rangle\langle 01| + |10\rangle\langle 10|, R_\perp = \sum_{s=1}^2 |r_s\rangle\langle r_s|, \quad (45)$$

where $\{|r_s\rangle\}$ is an orthonormal basis for $(\mathcal{V}^{0_L} \oplus \mathcal{V}^{1_L})^\perp$. A suitable basis $\mathcal{B}_{(\mathcal{V}^{0_L} \oplus \mathcal{V}^{1_L})^\perp}$ is given by,

$$\mathcal{B}_{(\mathcal{V}^{0_L} \oplus \mathcal{V}^{1_L})^\perp} = \{r_1 = |00\rangle, r_2 = |11\rangle\}. \quad (46)$$

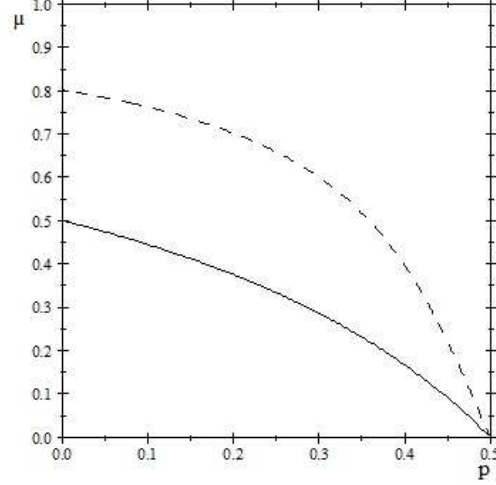


FIG. 1: Threshold curves for code effectiveness: concatenated code (dashed line), DFS (solid line). The concatenated code works in the parametric region below the dashed line. The DFS works in the region above the solid line. The repetition code works for any value of μ when $p \leq 0.5$.

The action of this recovery operation \mathcal{R} with $R_2 \equiv R_\perp$ on the map $\Lambda^{(2)}(\rho)$ in (37) yields,

$$\Lambda_{\text{recover}}^{(2)}(\rho) \equiv (\mathcal{R} \circ \Lambda^{(2)})(\rho) \stackrel{\text{def}}{=} \sum_{k=0}^3 \sum_{l=1}^2 (R_l A'_k) \rho (R_l A'_k)^\dagger. \quad (47)$$

We want to describe the action of $\mathcal{R} \circ \Lambda^{(2)}$ restricted to the code subspace \mathcal{C} . Therefore, we compute the 2×2 matrix representation $[R_l A'_k]_{|\mathcal{C}}$ of each $R_l A'_k$ with $l = 1, 2$ and $k = 0, \dots, 3$ where,

$$[R_l A'_k]_{|\mathcal{C}} \stackrel{\text{def}}{=} \begin{pmatrix} \langle 0_L | R_l A'_k | 0_L \rangle & \langle 0_L | R_l A'_k | 1_L \rangle \\ \langle 1_L | R_l A'_k | 0_L \rangle & \langle 1_L | R_l A'_k | 1_L \rangle \end{pmatrix}. \quad (48)$$

Substituting (38) and (45) into (48), it turns out that the only matrices $[R_l A'_k]_{|\mathcal{C}}$ with non-vanishing trace are given by,

$$[R_1 A'_0]_{|\mathcal{C}} = \sqrt{\tilde{p}_0^{(2)}} \begin{pmatrix} 1 & 0 \\ 0 & 1 \end{pmatrix}, \quad [R_1 A'_3]_{|\mathcal{C}} = -\sqrt{\tilde{p}_3^{(2)}} \begin{pmatrix} 1 & 0 \\ 0 & 1 \end{pmatrix} \quad (49)$$

Therefore, the entanglement fidelity $\mathcal{F}_{DFS}^{(2)}(\mu, p)$ defined in (10) results,

$$\mathcal{F}_{DFS}^{(2)}(\mu, p) = \mu(-2p^2 + 2p) + (2p^2 - 2p + 1). \quad (50)$$

We point out that error correction schemes improve the transmission accuracy only if the failure probability $\mathcal{P}(\mu, p)$ is strictly less than the error probability p [32],

$$\mathcal{P}(\mu, p) \stackrel{\text{def}}{=} 1 - \mathcal{F}(\mu, p) < p. \quad (51)$$

The threshold curves for code effectiveness $\bar{\mu}(p)$ are defined by the relation $1 - \mathcal{F}(\bar{\mu}(p), p) = 0$. They allow to select the two-dimensional parametric region where error correction schemes are useful. The threshold curve for the DFS for the model appears in Figure 1. The DFS works only in the parametric region above the thin solid line in Figure 1, while the repetition code works for all values of the memory degree μ when the error probability p is less than 0.5.

Concatenated Code. Following the line of reasoning presented in [33], we consider the concatenation of the two codes just described. In the case of (16) with $n = 6$ qubits and correlated errors in a dephasing quantum channel,

$$\Lambda^{(6)}(\rho) \stackrel{\text{def}}{=} \sum_{i_1, \dots, i_6=0}^1 p_{i_6|i_5} p_{i_5|i_4} p_{i_4|i_3} p_{i_3|i_2} p_{i_2|i_1} p_{i_1} (A_{i_6} A_{i_5} A_{i_4} A_{i_3} A_{i_2} A_{i_1}) \rho (A_{i_6} A_{i_5} A_{i_4} A_{i_3} A_{i_2} A_{i_1})^\dagger, \quad (52)$$

The error superoperator \mathcal{A} associated to channel (52) is defined in terms of the following error operators,

$$\mathcal{A} \longleftrightarrow \{A'_0, \dots, A'_{63}\} \text{ with } \Lambda^{(6)}(\rho) \stackrel{\text{def}}{=} \sum_{k=0}^{2^6-1} A'_k \rho A_k'^{\dagger} \text{ and, } \sum_{k=0}^{2^6-1} A_k'^{\dagger} A'_k = I_{64 \times 64}. \quad (53)$$

The error operators in the Kraus decomposition (53) are $\sum_{k=0}^6 \binom{6}{k} = 2^6 = 64$, where $\binom{6}{k}$ is the cardinality of weight- k error operators.

We encode our logical qubit with a concatenated subspace obtained by combining the decoherence free subspace in (40) (inner code, $\mathcal{C}_{DFS} = \mathcal{C}_{\text{inner}}$) with the repetition code in (23) (outer code, $\mathcal{C}_{\text{phase}} = \mathcal{C}_{\text{outer}}$). We obtain that the codewords of the concatenated code $\mathcal{C} = \mathcal{C}_{DFS} \circ \mathcal{C}_{\text{phase}}$ are given by,

$$|0_L\rangle \stackrel{\text{def}}{=} |++++--\rangle, \quad |1_L\rangle \stackrel{\text{def}}{=} |--++--\rangle. \quad (54)$$

Recall that the detectability condition is given by $P_C A'_k P_C = \lambda_{A'_k} P_C$ where the projector operator on the code space \mathcal{C} is $P_C = |0_L\rangle\langle 0_L| + |1_L\rangle\langle 1_L|$. Observe that,

$$P_C A'_k P_C = \langle 0_L | A'_k | 0_L \rangle |0_L\rangle\langle 0_L| + \langle 0_L | A'_k | 1_L \rangle |0_L\rangle\langle 1_L| + \langle 1_L | A'_k | 0_L \rangle |1_L\rangle\langle 0_L| + \langle 1_L | A'_k | 1_L \rangle |1_L\rangle\langle 1_L|. \quad (55)$$

Therefore, it turns out that for detectable error operators we must have,

$$\langle 0_L | A'_k | 0_L \rangle = \langle 1_L | A'_k | 1_L \rangle \text{ and, } \langle 0_L | A'_k | 1_L \rangle = \langle 1_L | A'_k | 0_L \rangle = 0. \quad (56)$$

In the case under consideration, it follows that the only error operator (omitting for the sake of simplicity the proper error amplitudes) not fulfilling the above conditions is proportional to,

$$Z^1 Z^2 Z^3 Z^4 Z^5 Z^6. \quad (57)$$

For such operator, we get

$$\langle 0_L | Z^1 Z^2 Z^3 Z^4 Z^5 Z^6 | 1_L \rangle = 1 \neq 0 \text{ and, } \langle 1_L | Z^1 Z^2 Z^3 Z^4 Z^5 Z^6 | 0_L \rangle = 1 \neq 0. \quad (58)$$

Therefore $Z^1 Z^2 Z^3 Z^4 Z^5 Z^6$ is not detectable. Thus, the cardinality of the set of detectable errors $\mathcal{A}_{\text{detectable}}$ is 63. Furthermore, recall that the set of correctable errors $\mathcal{A}_{\text{correctable}}$ is such that $\mathcal{A}_{\text{correctable}}^{\dagger} \mathcal{A}_{\text{correctable}}$ is detectable (in the hypothesis of invertible error operators). Therefore, after some reasoning, we conclude that the set of correctable errors is composed by 32 error operators. The correctable weight-0, 1 and 2 correctable error operators are (omitting the proper error amplitudes),

$$\{I\}_{\text{weight-0}}, \quad \{Z^1, Z^2, Z^3, Z^4, Z^5, Z^6\}_{\text{weight-1}}, \quad (59)$$

and,

$$\{Z^1 Z^2, Z^1 Z^3, Z^1 Z^4, Z^1 Z^5, Z^1 Z^6, Z^2 Z^3, Z^2 Z^4, Z^2 Z^5, Z^2 Z^6, Z^3 Z^4, Z^3 Z^5, Z^3 Z^6, Z^4 Z^5, Z^4 Z^6, Z^5 Z^6\}_{\text{weight-2}}, \quad (60)$$

respectively. The correctable weight-3 errors are,

$$\{Z^1 Z^3 Z^5, Z^1 Z^3 Z^6, Z^1 Z^4 Z^5, Z^1 Z^4 Z^6, Z^1 Z^5 Z^6, Z^2 Z^3 Z^4, Z^2 Z^3 Z^5, Z^2 Z^3 Z^6, Z^2 Z^4 Z^5, Z^2 Z^4 Z^6\}_{\text{weight-3}}. \quad (61)$$

There are no weight-4, 5 and 6 correctable error operators. The action of the correctable errors on the codewords in (54) is such that the Hilbert space \mathcal{H}_2^6 can be decomposed in two 32-dimensional orthogonal subspaces \mathcal{V}^{0_L} and \mathcal{V}^{1_L} . In other words, $\mathcal{H}_2^6 = \mathcal{V}^{0_L} \oplus \mathcal{V}^{1_L}$ where

$$\mathcal{V}^{0_L} = \text{Span} \left\{ |v_{k+1}^{0_L}\rangle = \frac{1}{\sqrt{\tilde{p}_k^{(6)}}} A'_k |0_L\rangle \right\} \text{ and, } \mathcal{V}^{1_L} = \text{Span} \left\{ |v_{k+1}^{1_L}\rangle = \frac{1}{\sqrt{\tilde{p}_k^{(6)}}} A'_k |1_L\rangle \right\}, \quad (62)$$

with $A'_k \in \mathcal{A}_{\text{correctable}} \forall k = 0, \dots, 31$ (numbering the correctable error operators from 0 to 31). Notice that $\langle v_k^{i_L} | v_{k'}^{j_L} \rangle = \delta_{kk'} \delta_{ij}$, with $k, k' \in \{0, \dots, 31\}$ and $i, j \in \{0, 1\}$ since,

$$\langle v_k^{i_L} | v_{k'}^{j_L} \rangle = \left\langle i_L \left| \frac{A_{k-1}'^{\dagger}}{\sqrt{\tilde{p}_k^{(6)}}} \frac{A_{k'-1}'}{\sqrt{\tilde{p}_{k'}^{(6)}}} \right| j_L \right\rangle = \frac{1}{\sqrt{\tilde{p}_k^{(6)} \tilde{p}_{k'}^{(6)}}} \langle i_L | A_k'^{\dagger} A_{k'}' | j_L \rangle = \frac{1}{\sqrt{\tilde{p}_k^{(6)} \tilde{p}_{k'}^{(6)}}} \alpha'_{kk'} \delta_{ij} = \delta_{kk'} \delta_{ij}, \quad (63)$$

where we have used the fact that the square (Hermitian) matrix $\alpha'_{kk'}$ equals $\sqrt{\tilde{p}_k^{(6)} \tilde{p}_{k'}^{(6)}} \delta_{kk'}$. The recovery superoperator $\mathcal{R} \leftrightarrow \{R_l\}$ with $l = 1, \dots, 32$ is defined as [31],

$$R_l \stackrel{\text{def}}{=} V_l \sum_{i=0}^1 |v_l^{iL}\rangle \langle v_l^{iL}|, \quad (64)$$

where the unitary operator V_l is such that $V_l |v_l^{iL}\rangle = |i_L\rangle$ for $i \in \{0, 1\}$. Notice that,

$$R_l \stackrel{\text{def}}{=} V_l \sum_{i=0}^1 |v_l^{iL}\rangle \langle v_l^{iL}| = |0_L\rangle \langle v_l^{0L}| + |1_L\rangle \langle v_l^{1L}|. \quad (65)$$

It turns out that the 32 recovery operators are given by,

$$R_{l+1} = R_l \frac{A'_l}{\sqrt{\tilde{p}'_l}} = (|0_L\rangle \langle 0_L| + |1_L\rangle \langle 1_L|) \frac{A'_l}{\sqrt{\tilde{p}'_l}}, \quad (66)$$

with $l \in \{0, \dots, 31\}$. Finally, the action of this recovery operation \mathcal{R} on the map $\Lambda^{(6)}(\rho)$ in (53) leads to,

$$\Lambda_{\text{recover}}^{(6)}(\rho) \equiv \left(\mathcal{R} \circ \Lambda^{(6)} \right)(\rho) \stackrel{\text{def}}{=} \sum_{k=0}^{2^6-1} \sum_{l=1}^{32} (R_l A'_k) \rho (R_l A'_k)^\dagger. \quad (67)$$

We want to describe the action of $\mathcal{R} \circ \Lambda^{(6)}$ restricted to the code subspace \mathcal{C} . Recalling that $A'_l = A_l'^\dagger$, it turns out that,

$$\langle i_L | R_{l+1} A'_k | j_L \rangle = \frac{1}{\sqrt{\tilde{p}'_l}} \langle i_L | 0_L \rangle \langle 0_L | A_l'^\dagger A'_k | j_L \rangle + \frac{1}{\sqrt{\tilde{p}'_l}} \langle i_L | 1_L \rangle \langle 1_L | A_l'^\dagger A'_k | j_L \rangle. \quad (68)$$

We now need to compute the 2×2 matrix representation $[R_l A'_k]_{|\mathcal{C}}$ of each $R_l A'_k$ with $l = 0, \dots, 31$ and $k = 0, \dots, 2^6 - 1$ where,

$$[R_{l+1} A'_k]_{|\mathcal{C}} \stackrel{\text{def}}{=} \begin{pmatrix} \langle 0_L | R_{l+1} A'_k | 0_L \rangle & \langle 0_L | R_{l+1} A'_k | 1_L \rangle \\ \langle 1_L | R_{l+1} A'_k | 0_L \rangle & \langle 1_L | R_{l+1} A'_k | 1_L \rangle \end{pmatrix}. \quad (69)$$

For $l, k = 0, \dots, 31$, we note that $[R_{l+1} A'_k]_{|\mathcal{C}}$ becomes,

$$[R_{l+1} A'_k]_{|\mathcal{C}} = \begin{pmatrix} \langle 0_L | A_l'^\dagger A'_k | 0_L \rangle & 0 \\ 0 & \langle 1_L | A_l'^\dagger A'_k | 1_L \rangle \end{pmatrix} = \sqrt{\tilde{p}'_l} \delta_{lk} \begin{pmatrix} 1 & 0 \\ 0 & 1 \end{pmatrix}, \quad (70)$$

while for any pair (l, k) with $l = 0, \dots, 31$ and $k > 31$, it follows that,

$$\langle 0_L | R_{l+1} A'_k | 0_L \rangle + \langle 1_L | R_{l+1} A'_k | 1_L \rangle = 0. \quad (71)$$

We conclude that the only matrices $[R_l A'_k]_{|\mathcal{C}}$ with non-vanishing trace are given by $[R_{l+1} A'_l]_{|\mathcal{C}}$ with $l = 0, \dots, 31$ where,

$$[R_{l+1} A'_l]_{|\mathcal{C}} = \sqrt{\tilde{p}'_l} \begin{pmatrix} 1 & 0 \\ 0 & 1 \end{pmatrix}. \quad (72)$$

Therefore, the entanglement fidelity $\mathcal{F}_{\text{conc}}^{(6)}(\mu, p)$ defined in (10) becomes,

$$\begin{aligned} \mathcal{F}_{\text{conc}}^{(6)}(\mu, p) = & p_{00}^5 p_0 + 2p_{00}^4 p_{10} p_0 + 4p_{00}^3 p_{01} p_{10} p_0 + p_{00}^3 p_{10} p_{11} p_0 + 3p_{00}^2 p_{01} p_{10}^2 p_0 + \\ & + p_{00}^3 p_{01} p_{10} p_1 + 3p_{00}^2 p_{01} p_{10} p_{11} p_0 + 3p_{00} p_{01}^2 p_{10}^2 p_0 + 3p_{00}^2 p_{01}^2 p_{10} p_1 + p_{00}^3 p_{01} p_{11} p_1 + \\ & + p_{01}^2 p_{10}^3 p_0 + 2p_{00} p_{01}^2 p_{10}^2 p_1 + p_{00} p_{01} p_{10}^2 p_{11} p_0 + p_{00}^2 p_{01} p_{10} p_{11} p_1 + p_{00} p_{01} p_{10} p_{11}^2 p_0 + \\ & + 2p_{01}^2 p_{10}^2 p_{11} p_0 + p_{00} p_{01}^2 p_{10} p_{11} p_1 + p_{01}^3 p_{10}^2 p_1. \end{aligned} \quad (73)$$

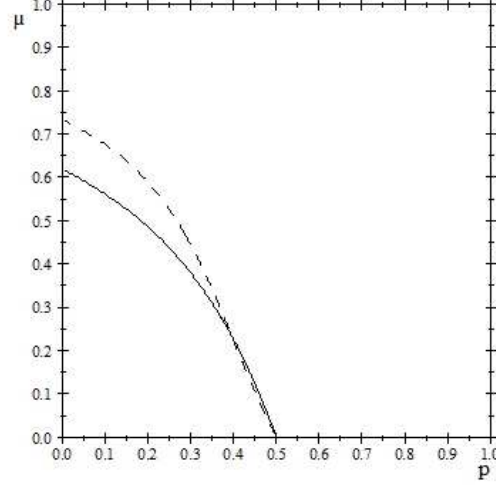


FIG. 2: Threshold curves for code performance: concatenated code vs. DFS (thin solid line) and concatenated code vs. repetition code (dashed line). The concatenated code outperforms the DFS in the parametric region below the solid line and outperforms the repetition code in the region below the dashed line.

Substituting (22) into (7), we finally get

$$\begin{aligned} \mathcal{F}_{\text{conc}}^{(6)}(\mu, p) = & \mu^5 (-4p^5 + 11p^4 - 10p^3 + 3p^2) + \mu^4 (10p^5 - 25p^4 + 22p^3 - 8p^2 + p) + \\ & + \mu^3 (-6p^4 + 12p^3 - 7p^2 + p) + \mu^2 (-20p^5 + 58p^4 - 60p^3 + 25p^2 - 3p) + \\ & + \mu (20p^5 - 53p^4 + 46p^3 - 13p^2) + (-6p^5 + 15p^4 - 10p^3 + 1). \end{aligned} \quad (74)$$

The threshold curve for code effectiveness concerning the concatenated code defined in (54) for our noise model appears in Figure 1. It turns out that the concatenated code works in the parametric region below the dashed line.

To uncover the parametric region where one code (say, code-1) outperforms another code (say, code-2), we consider the threshold curves for code performances $\bar{\mu}(p)$ defined by the relation $\mathcal{F}_{\text{code-1}}(\bar{\mu}(p), p) - \mathcal{F}_{\text{code-2}}(\bar{\mu}(p), p) = 0$. We emphasize that in view of equations (36), (50) and (74), it turns out that the concatenated code outperforms the DFS in the parametric region below the solid line ($\mathcal{F}_{\text{conc}}^{(6)}(\bar{\mu}(p), p) - \mathcal{F}_{\text{DFS}}^{(2)}(\bar{\mu}(p), p) = 0$) and outperforms the three-qubit repetition code in the region below the dashed line ($\mathcal{F}_{\text{conc}}^{(6)}(\bar{\mu}(p), p) - \mathcal{F}_{\text{phase}}^{(3)}(\bar{\mu}(p), p) = 0$) in Figure 2. For the sake of clarity, in Figure 3 we plot the entanglement fidelities (36) (thin solid line), (74) (dashed line) and (50) (thick solid line) for $p = 10^{-2}$. Our analysis explicitly shows that none of the two codes (DFS and repetition code) is effective in the extreme limit when the other is, the repetition code still works for correlated errors, whereas the error avoiding code does not work in the absence of correlations. Finally, our final finding leads to conclude that there is a parametric region characterized by intermediate values of the memory parameter where the concatenated code in (54) is particularly advantageous (see Figure 3).

B. Code entropy-based analysis

Repetition code for correlated phase flips. The error correction matrix Γ_{phase} for the three-qubit repetition code considered is given by,

$$\Gamma_{\text{phase}} = \begin{pmatrix} p_{00}^2 p_0 & 0 & 0 & 0 \\ 0 & p_{00} p_{10} p_0 & 0 & 0 \\ 0 & 0 & p_{01} p_{10} p_0 & 0 \\ 0 & 0 & 0 & p_{00} p_{01} p_1 \end{pmatrix}. \quad (75)$$

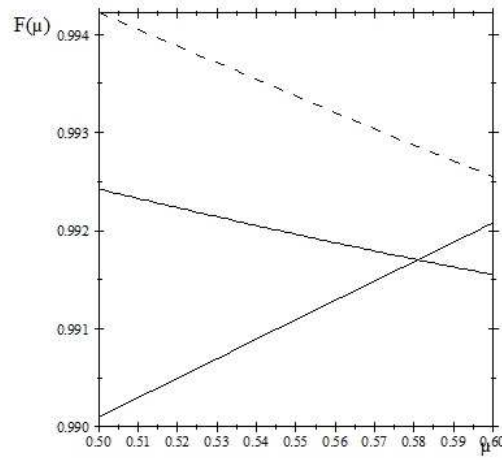


FIG. 3: Entanglement fidelity vs. memory parameter μ for $p = 10^{-2}$: concatenated code (dashed line), DFS (thick solid line) and repetition code (thin solid line).

Therefore the repetition code entropy $\mathcal{S}_{\text{RC}}(\mu, p)$ results from (14),

$$\mathcal{S}_{\text{RC}} = -p_{00}^2 p_0 \log_2(p_{00}^2 p_0) - p_{00} p_{10} p_0 \log_2(p_{00} p_{10} p_0) - p_{01} p_{10} p_0 \log_2(p_{01} p_{10} p_0) - p_{00} p_{01} p_1 \log_2(p_{00} p_{01} p_1), \quad (76)$$

with,

$$\begin{aligned} p_{00}^2 p_0 &= \mu^2 (-p^3 + p^2) + \mu (2p^3 - 4p^2 + 2p) + (-p^3 + 3p^2 - 3p + 1), \\ p_{00} p_{10} p_0 &= p_{00} p_{01} p_1 = \mu^2 (p^3 - p^2) + \mu (-2p^3 + 3p^2 - p) + (p^3 - 2p^2 + p), \\ p_{01} p_{10} p_0 &= \mu^2 (p^3 - 2p^2 + p) + \mu (-2p^3 + 4p^2 - 2p) + (p^3 - 2p^2 + p). \end{aligned} \quad (77)$$

In this case it turns out that there is no value of the memory parameter μ for which \mathcal{C}_{RC} is a unitarily correctable code. In other words, $\mathcal{S}_{\text{RC}}(\mu, p) \neq 0$ for any $0 \leq \mu \leq 1$ with $0 \leq p < 1$. Therefore, it never occurs the case where the effort for recovering the code is minimum. For instance, in the extreme limit of $\mu = 1$ it follows that $\mathcal{S}_{\text{RC}}(\mu = 1, p) = -(1-p) \log_2(1-p) \neq 0$. From Figure 4, we notice that in general in the limit of small error probabilities ($p \ll 1$), the nearness of \mathcal{C}_{RC} to a DFS increases when μ increases and/or the error probability p decreases. Therefore the RC entropy analysis, although not particularly enlightening, confirms that there is no pair of parametric values μ and p for which \mathcal{C}_{RC} provides a fully protected space in the presence of correlated phase-flip errors and the effort required for recovering the quantum state corrupted by the phase-flip noise increases when p increases.

DFS for correlated phase flips. The error correction matrix Γ_{DFS} for the DFS considered is given by,

$$\Gamma_{\text{DFS}} = \begin{pmatrix} a & c \\ c & b \end{pmatrix}, \quad (78)$$

where,

$$a \stackrel{\text{def}}{=} p_{00} p_0, \quad b \stackrel{\text{def}}{=} p_{11} p_1, \quad c \stackrel{\text{def}}{=} -\sqrt{p_{00} p_0 p_{11} p_1}. \quad (79)$$

Diagonalizing Λ_{DFS} , it turns out that,

$$[\Lambda_{\text{DFS}}]_{\text{diagonal}} = \begin{pmatrix} \lambda_+ & 0 \\ 0 & \lambda_- \end{pmatrix}, \quad (80)$$

with,

$$\lambda_{\pm} = \frac{1}{2} \left[(a + b) \pm \sqrt{(a - b)^2 + 4c^2} \right]. \quad (81)$$

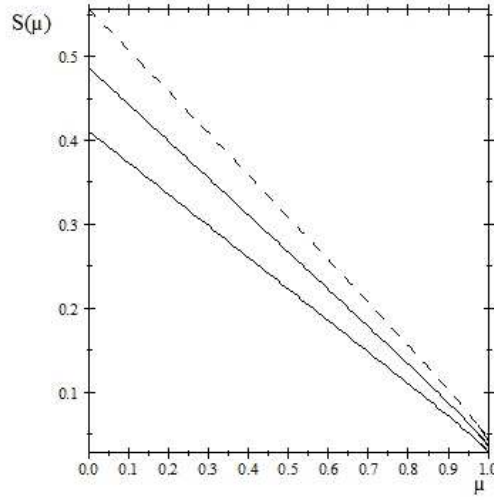


FIG. 4: RC entropy vs. μ for $p = 2 \times 10^{-2}$ (thick solid line), $p = 2.5 \times 10^{-2}$ (thin solid line) and $p = 3 \times 10^{-2}$ (dash line). The RC entropy does not vanish for $\mu = 1$.

Substituting (79) into (81) and recalling that,

$$\begin{aligned} p_0 &= (1-p), \quad p_1 = p, \quad p_{00} = ((1-\mu)(1-p) + \mu), \\ p_{01} &= (1-\mu)(1-p), \quad p_{10} = (1-\mu)p, \quad p_{11} = ((1-\mu)p + \mu), \end{aligned} \quad (82)$$

we obtain,

$$\lambda_+ = \mu(-2p^2 + 2p) + (2p^2 - 2p + 1) \quad \text{and} \quad \lambda_- = 0. \quad (83)$$

In conclusion the code entropy $\mathcal{S}_{\text{DFS}}(\mu, p)$ results from (14),

$$\mathcal{S}_{\text{DFS}}(\mu, p) = - [\mu(-2p^2 + 2p) + (2p^2 - 2p + 1)] \log_2 [\mu(-2p^2 + 2p) + (2p^2 - 2p + 1)]. \quad (84)$$

From Figure 4, it follows that \mathcal{C}_{DFS} is a unitarily correctable code only in the extreme limit of $\mu = 1$. In such a case, $\mathcal{S}_{\text{DFS}}(\mu = 1, p) = 0$ for any $0 \leq p \leq 1$ and thus the effort for recovering the code is minimum since a trivial identity recovery operation will do the job. From Figures 5 and 6, we notice that in general in the limit of small error probabilities ($p \ll 1$), the effort required for recovering the quantum state corrupted by the phase-flip noise increases when μ increases and/or p increases. Thus, the DFS entropy analysis leads to the conclusion that \mathcal{C}_{DFS} provides an especially useful error correction scheme for very small error probabilities and highly correlated phase-flip errors.

Concatenated Code. After some straightforward but tedious algebra, it turns out that the entropy of the concatenated code $\mathcal{S}_{\text{conc.}}(\mu, p)$ is given by,

$$\mathcal{S}_{\text{conc.}}(\mu, p) = - \sum_{j=0}^{31} f_j(\mu, p) \log_2 f_j(\mu, p), \quad (85)$$

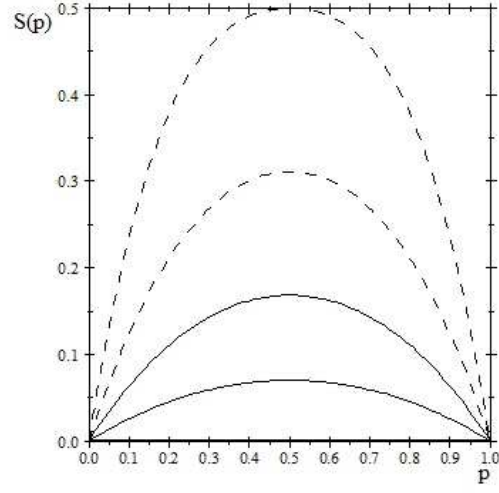


FIG. 5: DFS entropy vs. p for $\mu = 1$ (thick solid line), $\mu = 0.90$ (medium solid line), $\mu = 0.75$ (thin solid line), $\mu = 0.5$ (thick dash line) and $\mu = 0$ (thin dash line).

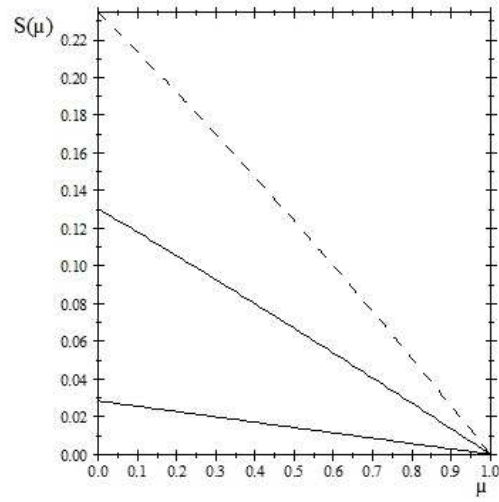


FIG. 6: DFS entropy vs. memory parameter for $p = 10^{-1}$ (dash solid line), $p = 5 \times 10^{-2}$ (thin solid line) and $p = 10^{-2}$ (medium solid line). The DFS entropy vanishes for $\mu = 1$.

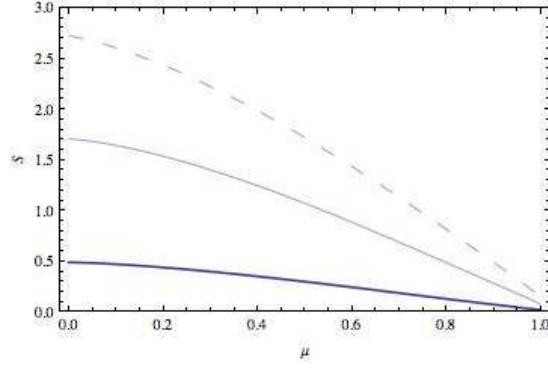


FIG. 7: Concatenated code entropy vs. memory parameter μ for $p = 10^{-1}$ (dashed solid line), $p = 5 \times 10^{-2}$ (thin solid line), $p = 10^{-2}$ (medium solid line),

where,

$$\begin{aligned}
 f_0 &= p_{00}^5 p_0, f_1 = f_2 = p_{00}^4 p_{10} p_0, f_3 = f_4 = f_5 = f_6 = p_{00}^3 p_{01} p_{10} p_0, f_7 = p_{00}^3 p_{10} p_{11} p_0, \\
 f_8 &= f_9 = f_{10} = p_{00}^2 p_{01} p_{10}^2 p_0, f_{11} = p_{00}^3 p_{01} p_{10} p_1, f_{12} = f_{13} = f_{14} = p_{00}^2 p_{01} p_{10} p_{11} p_0, \\
 f_{15} &= f_{16} = f_{17} = p_{00} p_{01}^2 p_{10}^2 p_0, f_{18} = f_{19} = f_{20} = p_{00}^2 p_{01}^2 p_{10} p_1, f_{21} = p_{00}^3 p_{01} p_{11} p_1, \\
 f_{22} &= p_{01}^2 p_{10}^3 p_0, f_{23} = f_{24} = p_{00} p_{01}^2 p_{10}^2 p_1, f_{25} = p_{00} p_{01} p_{10}^2 p_{11} p_0, f_{26} = p_{00}^2 p_{01} p_{10} p_{11} p_1, \\
 f_{27} &= p_{00} p_{01} p_{10} p_{11}^2 p_0, f_{28} = f_{29} = p_{01}^2 p_{10}^2 p_{11} p_0, f_{30} = p_{00} p_{01}^2 p_{10} p_{11} p_1, f_{31} = p_{01}^3 p_{10}^2 p_1,
 \end{aligned} \tag{86}$$

and,

$$\begin{aligned}
 p_0 &= (1 - p), p_1 = p, p_{00} = ((1 - \mu)(1 - p) + \mu), \\
 p_{01} &= (1 - \mu)(1 - p), p_{10} = (1 - \mu)p, p_{11} = ((1 - \mu)p + \mu).
 \end{aligned} \tag{87}$$

It can be easily checked that in the extreme limit of $\mu = 1$ it follows that $\mathcal{S}_{\text{conc.}}(\mu = 1, p) = -(1 - p) \log_2(1 - p) \neq 0$. In general, it appears that results similar to those obtained within the RC code entropy analysis hold (see Figure 7). Then, it seems that the nearness of $\mathcal{C}_{\text{conc.}}$ to a DFS increases when μ increases and/or the error probability p decreases. In particular, the effort required for recovering the quantum state corrupted by the phase-flip noise increases when p increases.

Our analysis for Model I allows us to conclude that the entanglement fidelity is generally a better code performance quantifier than the code entropy since it is easier to handle computationally and, most of all, it allows to compare performances of different error correction techniques applied to the same error model in a smoother way. However, it appears that the code entropy is especially informative when quantifying the performance of DFSs in the limit of highly correlated and very low error probabilities.

IV. MODEL II: ASYMMETRIC DEPOLARIZING NOISY QUANTUM MEMORY CHANNEL

In this Section, we consider both symmetric and asymmetric depolarizing noisy quantum memory channels and perform quantum error correction via the five qubit stabilizer code $\mathcal{C}_{[[5,1,3]]}$. We characterize this code by means of the code entropy and the entanglement fidelity as function of the error probability and the degree of memory. In particular, we uncover that while asymmetric depolarizing errors do not affect the entanglement fidelity of the five qubit code, they do affect its code entropy.

A. Entanglement fidelity-based analysis

For the symmetric case, consider five qubits and Markov correlated errors in a depolarizing quantum channel $\Lambda^{(5)}(\rho)$,

$$\Lambda^{(5)}(\rho) = \sum_{i_1, i_2, i_3, i_4, i_5=0}^3 p_{i_5|i_4} p_{i_4|i_3} p_{i_3|i_2} p_{i_2|i_1} p_{i_1} \left[A_{i_5} A_{i_4} A_{i_3} A_{i_2} A_{i_1} \rho A_{i_1}^\dagger A_{i_2}^\dagger A_{i_3}^\dagger A_{i_4}^\dagger A_{i_5}^\dagger \right], \quad (88)$$

where $A_0 \equiv I$, $A_1 \equiv X$, $A_2 \equiv Y$, $A_3 \equiv Z$ are the Pauli operators. The coefficients $p_{i_l|i_m}$ (conditional probabilities) with $l, m \in \{0, 1, \dots, 5\}$ satisfy the normalization condition,

$$\sum_{i_1, i_2, i_3, i_4, i_5=0}^3 p_{i_5|i_4} p_{i_4|i_3} p_{i_3|i_2} p_{i_2|i_1} p_{i_1} = 1. \quad (89)$$

For the depolarizing channel $\Lambda^{(5)}(\rho)$, coefficients $p_{i_l|i_m}$ are considered as,

$$p_{k|k-1} \stackrel{\text{def}}{=} (1 - \mu)p_k + \mu\delta_{k|k-1}, \quad p_{k=0} = 1 - p, \quad p_{k=1, 2, 3} = p/3. \quad (90)$$

Following [11], it turns out that the entanglement fidelity $\mathcal{F}_{\text{symmetric}}^{[[5,1,3]]}(\mu, p)$ results from (10)

$$\mathcal{F}_{\text{symmetric}}^{[[5,1,3]]}(\mu, p) = \sum_{k=0}^{15} f_k(\mu, p) = f_0 + (f_1 + \dots + f_6) + (f_7 + \dots + f_{15}), \quad (91)$$

where the functions $f_k(\mu, p)$ are given by,

$$f_0 = p_{00}^4 p_0, \quad f_1 = \dots = f_6 = p_{00}^3 p_{10} p_0, \quad f_7 = \dots = f_{15} = p_{00}^2 p_{01} p_{10} p_0, \quad (92)$$

with,

$$\begin{aligned} p_0 &= 1 - p, \quad p_1 = p_2 = p_3 = \frac{p}{3}, \quad p_{00} = (1 - \mu)(1 - p) + \mu, \\ p_{01} &= p_{02} = p_{03} = (1 - \mu)(1 - p), \quad p_{10} = p_{20} = p_{30} = \frac{p}{3}(1 - \mu). \end{aligned} \quad (93)$$

For the asymmetric case, we assume that the error probability p may be written as,

$$p = p_X + p_Y + p_Z, \quad (94)$$

where,

$$p_X = \alpha_X p, \quad p_Y = \alpha_Y p, \quad p_Z = \alpha_Z p, \quad (95)$$

with $\alpha_X + \alpha_Y + \alpha_Z = 1$. Notice that in the symmetric case, we simply have $\alpha_X = \alpha_Y = \alpha_Z = \frac{1}{3}$. It turns out that the $\mathcal{F}_{\text{asymmetric}}^{[[5,1,3]]}(\mu, p)$ is given by [11],

$$\mathcal{F}_{\text{asymmetric}}^{[[5,1,3]]}(\mu, p; \alpha_X, \alpha_Y, \alpha_Z) = \sum_{k=0}^{15} f'_k(\mu, p; \alpha_X, \alpha_Y, \alpha_Z) = f'_0 + (f'_1 + \dots + f'_6) + (f'_7 + \dots + f'_{15}), \quad (96)$$

where the functions $f'_k(\mu, p; \alpha_X, \alpha_Y, \alpha_Z)$ read,

$$\begin{aligned} f'_0 &= p_{00}^4 p_0, \quad f'_1 = p_{00}^3 p_{01} p_0, \quad f'_2 = p_{00}^3 p_{02} p_0, \quad f'_3 = p_{00}^3 p_{03} p_0, \quad f'_4 = p_{00}^3 p_{01} p_1, \quad f'_5 = p_{00}^3 p_{01} p_2, \quad f'_6 = p_{00}^3 p_{01} p_3, \\ f'_7 &= f'_8 = f'_9 = p_{00}^2 p_{01} p_{10} p_0, \quad f'_{10} = f'_{11} = f'_{12} = p_{00}^2 p_{01} p_{20} p_0, \quad f'_{13} = f'_{14} = f'_{15} = p_{00}^2 p_{01} p_{30} p_0, \end{aligned} \quad (97)$$

with,

$$\begin{aligned} p_0 &= 1 - p, \quad p_1 = \alpha_X p, \quad p_2 = \alpha_Y p, \quad p_3 = \alpha_Z p, \quad p_{00} = (1 - \mu)(1 - p) + \mu, \\ p_{01} &= p_{02} = p_{03} = (1 - \mu)(1 - p), \quad p_{10} = \alpha_X p(1 - \mu), \quad p_{20} = \alpha_Y p(1 - \mu), \quad p_{30} = \alpha_Z p(1 - \mu). \end{aligned} \quad (98)$$

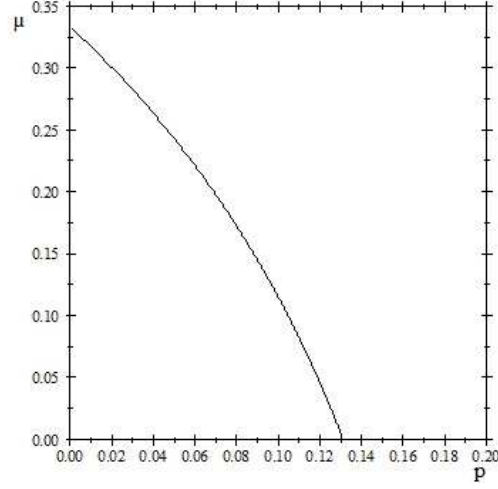


FIG. 8: Threshold curve for the five-qubit stabilizer code effectiveness. The $\mathcal{C}_{[[5,1,3]]}$ code works in the parametric region below the curve.

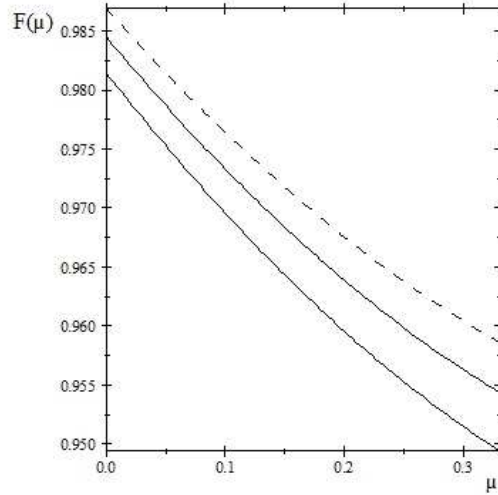


FIG. 9: $\mathcal{F}^{[[5,1,3]]}(\mu)$ vs. μ with $0 \leq \mu \leq 0.33$ (for $\mu > 0.33$, the error correction scheme is not effective anymore) for $p = 4.50 \times 10^{-2}$ (thick solid line), $p = 4.10 \times 10^{-2}$ (thin solid line) and $p = 3.75 \times 10^{-2}$ (dashed line).

Recalling that in the symmetric case $p_1 = p_2 = p_3 = \frac{p}{3}$ and $p_{10} = p_{20} = p_{30} = \frac{p}{3}(1 - \mu)$ and substituting (98) in (96), it follows that

$$\mathcal{F}_{\text{asymmetric}}^{[[5,1,3]]}(\mu, p; \alpha_X, \alpha_Y, \alpha_Z) = \mathcal{F}_{\text{symmetric}}^{[[5,1,3]]}(\mu, p). \quad (99)$$

Therefore, we conclude that the performance of the five-qubit stabilizer code, when quantified by the entanglement fidelity, remains unaffected by the asymmetry of the depolarizing error probabilities. From (96) it can be shown that such error correction scheme only works for low values of μ (see Figure 8). Furthermore, it also turns out that the performance of the five qubit quantum stabilizer code is lowered by increasing values of the degree of memory μ and increasing values of the error probability values p (see Figure 9). For a more detailed overview of such findings, we refer to [11].

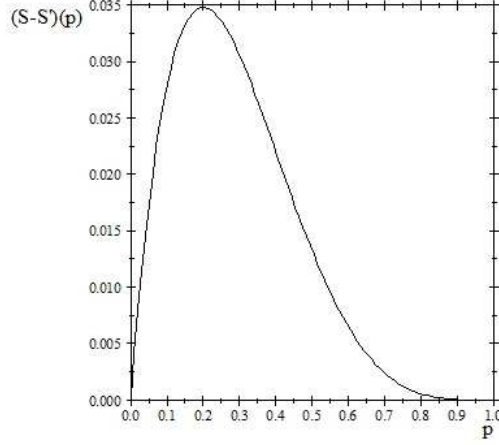


FIG. 10: Difference between the five qubit stabilizer code entropies $\mathcal{S}_{\text{symmetric}}^{[[5,1,3]]}(p)$ and $\mathcal{S}_{\text{asymmetric}}^{[[5,1,3]]}(p)$ in the absence of correlations ($\mu = 0$) with $\alpha_x = \alpha_y = \frac{1}{4}$ and $\alpha_z = \frac{1}{2}$.

B. Code entropy-based analysis

Omitting technical details and following the work presented in the previous Section, it turns out that the five qubit code entropies for the symmetric and asymmetric depolarizing quantum memory channels are given by,

$$\mathcal{S}_{\text{symmetric}}^{[[5,1,3]]}(\mu, p) = - \sum_{j=0}^{15} f_j(\mu, p) \log_2 f_j(\mu, p), \quad (100)$$

and,

$$\mathcal{S}_{\text{asymmetric}}^{[[5,1,3]]}(\mu, p; \alpha_X, \alpha_Y, \alpha_Z) = - \sum_{j=0}^{15} f'_j(\mu, p; \alpha_X, \alpha_Y, \alpha_Z) \log_2 f'_j(\mu, p; \alpha_X, \alpha_Y, \alpha_Z), \quad (101)$$

respectively. The explicit expressions for the functions $f_j(\mu, p)$ and $f'_j(\mu, p; \alpha_X, \alpha_Y, \alpha_Z)$ are given in (92) and (97), respectively. From (100) and (101), it can be shown that

$$\mathcal{S}_{\text{symmetric}}^{[[5,1,3]]}(\mu, p) \neq \mathcal{S}_{\text{asymmetric}}^{[[5,1,3]]}(\mu, p; \alpha_X, \alpha_Y, \alpha_Z). \quad (102)$$

Numerical evidence of the disequality in (102) can be easily verified at least for a suitable choice of model parameters μ , α_X , α_Y and α_Z . In Figure 10, we plot the change of the five qubit code entropy $\Delta_S(p)$ as function of the error probability p . Specifically, $\Delta_S(p)$ is the difference between the five qubit code entropies $\mathcal{S}_{\text{symmetric}}^{[[5,1,3]]}(p)$ and $\mathcal{S}_{\text{asymmetric}}^{[[5,1,3]]}(p)$ in the absence of correlations ($\mu = 0$) with $\alpha_x = \alpha_y = \frac{1}{4}$ and $\alpha_z = \frac{1}{2}$. The positivity of $\Delta_S(p)$ leads to conclude that when the error model considered is defined by a suitable choice of numerical values of the model parameters, it can happen that the effort required for recovering the five qubit code in the asymmetric case is less than in the symmetric case. This scenario never occurs when quantifying the performance of the five qubit code applied to asymmetric and correlated depolarizing errors by means of the entanglement fidelity.

From an analytical point of view, (102) can be readily understood by noticing that $\mathcal{S}_{\text{symmetric}}^{[[5,1,3]]}(\mu, p)$ in (100) and $\mathcal{S}_{\text{asymmetric}}^{[[5,1,3]]}(\mu, p; \alpha_X, \alpha_Y, \alpha_Z)$ in (101) are sums of terms that are *nonlinear* in the functions (amplitude square probabilities of the correctable error operators) $f_j(\mu, p)$ and $f'_j(\mu, p; \alpha_X, \alpha_Y, \alpha_Z)$, respectively. As a matter of fact it turns out that,

$$\sum_{k=0}^{15} f_k = \sum_{k=0}^{15} f'_k, \quad (103)$$

with $f'_0 = f_0 = p_{00}^4 p_0$, $f'_1 + \dots + f'_6 = f_1 + \dots + f_6$, $f'_7 + \dots + f'_{15} = f_7 + \dots + f_{15}$ and, $f'_i \neq f'_j$ for $i, j = 1, \dots, 6$; $f'_7 = f'_8 = f'_9 = p_{00}^2 p_{01} p_0 p_{10}$; $f'_{10} = f'_{11} = f'_{12} = p_{00}^2 p_{01} p_0 p_{20}$ and $f'_{13} = f'_{14} = f'_{15} = p_{00}^2 p_{01} p_0 p_{30}$. However, the constraint in (103) together with the nonlinearity in f and f' characterizing the expressions of the code entropies in (100) and (101) imply that,

$$\sum_{k=0}^{15} f_k \log_2 f_k \neq \sum_{k=0}^{15} f'_k \log_2 f'_k. \quad (104)$$

In conclusion, since the entanglement fidelity is a linear combination of the amplitude square probabilities of the correctable error operators, Eq. (103) holds true, and the equality in (99) is proven. On the contrary, the code entropy is a *nonlinear* combination of the amplitude square probabilities and the use of (104) leads naturally to the inequality in (102).

Therefore, we conclude that the performance of the five-qubit stabilizer code, when quantified by the code entropy and not by the entanglement fidelity, does remain affected by the asymmetry of the depolarizing error probabilities. Our finding provides a neat quantitative manifestation of the conceptual fact [26] that no single code performance quantifier holds all the information on a code.

V. FINAL REMARKS

In this article, we studied the properties of error correcting codes for noise models in the presence of asymmetries and/or correlations by means of the entanglement fidelity and the code entropy. We considered a dephasing Markovian memory channel (Model I) and both symmetric and asymmetric depolarizing quantum memory channels (Model II). For each model, we presented both an entanglement fidelity-based and a code entropy-based analyses. For Model I, we used three codes: the repetition code \mathcal{C}_{RC} , the DFS \mathcal{C}_{DFS} and the concatenated code $\mathcal{C}_{DFS} \circ \mathcal{C}_{RC}$. For Model II, we employed the five qubit stabilizer code $\mathcal{C}_{[[5,1,3]]}$.

For Model I, the entanglement fidelity-based analysis allows to find out the parametric regions where the chosen error correction schemes are effective (see Figure 1). This analysis is also suitable to determine where, within such parametric regions, one code outperforms the other (see Figure 2). In particular, we showed that the concatenated code quantified by the entanglement fidelity is useful to combat partially correlated phase-flip errors (see Figure 3). The code entropy-based analysis for Model I leads to the conclusion that the effort required for recovering the quantum state corrupted by correlated phase-flip errors increases when the memory parameter μ decreases and the error probability p increases (see Figures 4 and 6). Furthermore, it turns out that only \mathcal{C}_{DFS} is a unitarily correctable code for the noise model considered in the limiting case of $\mu = 1$ (see Figure 5). When applied to the concatenated code, the code entropy-based analysis is not as enlightening as the entanglement-fidelity based analysis. It is not particularly useful for drawing performance comparisons with the repetition code (see Figure 7).

For Model II, the entanglement fidelity-based analysis allows us to find out that the five qubit stabilizer code only works for small values of μ (see Figure 8). Furthermore, the performance of this code applied to symmetric and asymmetric correlated depolarizing errors is lowered by increasing values of the memory parameter μ and increasing values of the error probability p (see Figure 9). Finally, the code entropy-based analysis applied to Model II leads to an interesting result. While asymmetry in the depolarizing errors does not affect in any case the performance of the five qubit stabilizer code quantified by means of the entanglement fidelity, it may affect positively the performance of $\mathcal{C}_{[[5,1,3]]}$ by lowering the effort required for recovering the code subjected to asymmetric depolarizing errors (see Figure 10).

Although our work is limited to only few error models in the presence of correlations and asymmetry and we only perform error correction by means of few quantum codes, we feel we have gathered enough evidence to draw the following conclusions on the code performance quantifiers employed: a) while the code entropy may capture new undetected features of a code with respect to those encoded into the entanglement fidelity and deserves further investigations, it is certainly harder to compute for realistic physical models and non-trivial quantum codes; b) the code entropy seems to lack the reliability and practicality characterizing the entanglement fidelity.

In summary, the entropy of a code appears to be an interesting auxiliary tool for quantifying the code performances. In particular, it is our intention to explore in future investigations the possibility of devising a hybrid code performance quantifier whose nonlinear structure in the amplitude square probabilities of the correctable error operators may not be necessarily characterized by the logarithmic behavior which identifies the code entropy. For the time being, motivated by our analysis and in agreement with [24, 34, 35], we believe that the entanglement fidelity remains the most relevant tool to maximize in schemes for quantum error correction.

Acknowledgments

The research leading to these results has received funding from the European Commission's Seventh Framework Programme (FP7/2007–2013) under grant agreements no. 213681.

-
- [1] Gottesman, D., An Introduction to Quantum Error Correction and Fault-Tolerant Quantum Computation, in *Quantum Information Science and Its Contributions to Mathematics, Proceedings of Symposia in Applied Mathematics*, Amer. Math. Soc., Providence, Rhode Island, 2010, 13-58.
 - [2] Lidar, D. A. and Whaley, K. B., Decoherence-Free Subspaces and Subsystems, in: F. Benatti and R. Floreanini, (eds.), *Irreversible Quantum Dynamics*, Springer Lecture Notes in Physics, Berlin, 2003, 83-120.
 - [3] Garg, A., *Phys. Rev. Lett.* **77** (1996), 964.
 - [4] Loss, D. and Di Vincenzo, D. P., *Phys. Rev. A* **57** (1998), 120.
 - [5] Hwang, W. Y., Ahn, D. and Hwang, S. W., *Phys. Rev. A* **63** (2001), 022303.
 - [6] Clemens, J. P., Siddiqui, S. and Gea-Banacloche, J., *Phys. Rev. A* **69** (2004), 062313.
 - [7] Klesse, R. and Frank, S., *Phys. Rev. Lett.* **95** (2005), 230503.
 - [8] Shabani, A. *Phys. Rev. A* **77** (2008), 022323.
 - [9] D'Arrigo, A., De Leo, E., Benenti, G., Falcì, G., *Int. J. Quantum Inf.* **6** (2008), 651.
 - [10] Cafaro, C. and Mancini, S., *Phys. Lett. A* **374** (2010), 2688.
 - [11] Cafaro, C. and Mancini, S., *Phys. Rev. A* **82** (2010), 012306.
 - [12] Astafiev, O., Pashkin, Yu. A., Nakamura, Y., Yamamoto, T. and Tsai, J. S., *Phys. Rev. Lett.* **93** (2004), 267007.
 - [13] Ioffe, L. and Mezard, M. *Phys. Rev. A* **75** (2007), 032345.
 - [14] Evans, Z. W. E., Stephens, A. M., Cole, J. H., Hollenberg, L. C. L., arXiv:quant-ph/0709.3875 (2007).
 - [15] Stephens, A. M., Evans, Z. W. E., Devitt, S. J. and Hollenberg, L. C. L. *Phys. Rev. A* **77** (2008), 062335.
 - [16] Sarvepalli, P. K., Roetteler, M., Klappenecker, A., arXiv:quant-ph/0804.4316 (2008).
 - [17] Aly, S. A., arXiv:quant-ph/0803.0764 (2008).
 - [18] Gottesman, D., arXiv:quant-ph/9607027 (1996).
 - [19] Calderbank, R. A., Rains, E., Shor, P. and Sloane, N., *IEEE Trans. Inf. Theor.* **44** (1998), 1369.
 - [20] Forney, G. D. Jr., *Concatenated Codes*, MIT Press, Cambridge, 1966.
 - [21] Gottesman, D., *Stabilizer codes and quantum error correction*, Caltech Ph.D. Thesis (1997), arXiv:quant-ph/9705052.
 - [22] Knill, E. and Laflamme, R., arXiv:quant-ph/9608012 (1996).
 - [23] Nielsen, M. A. and Chuang, I. L. *Quantum Computation and Information*, Cambridge University Press, Cambridge, 2000.
 - [24] Nielsen, M. A., arXiv: quant-ph/9606012 (1996).
 - [25] Schumacher, B., *Phys. Rev. A* **54** (1996), 2615.
 - [26] Kribs, D.W., Pasieka, A., Zyczkowski, K., *Open Syst. Inf. Dyn.* **15** (2008), 329.
 - [27] Majgier, K., Maassen, H., Zyczkowski, K., *Quantum Inf. Process.* **3** (2010), 343.
 - [28] Lindblad, G., *Quantum entropy and quantum measurements*, Lecture Notes in Physics **378** (1991), 36.
 - [29] Kaye, P., Laflamme R., Mosca, M., *An Introduction to Quantum Computing*, Oxford University Press, Oxford, 2007.
 - [30] Knill, E., Laflamme, R., Ashikhmin, A., Barnum, H., Viola, L., Zurek, W.H., arXiv:quant-ph/020717 (2002).
 - [31] Knill, E. and Laflamme, R., *Phys. Rev. A* **55** (1997), 900.
 - [32] Gaitan, F., *Quantum Error Correction and Fault Tolerant Quantum Computing*, CRC Press, 2008.
 - [33] Cafaro, C. and Mancini, S., arXiv:quant-ph/1006.2051 (2010).
 - [34] Cory, D., Price, M. D., Maas, W., Knill, E., Laflamme, R., Zurek, W. H., Havel, T. F. and Somaroo, S. S., *Phys. Rev. Lett.* **81** (1998), 2152.
 - [35] Knill, E., Laflamme, R., Martinez, R. and Negrevergne, C., *Phys. Rev. Lett.* **86** (2001), 5811.